Proc. Natl. Acad. Sci. USA
Vol. 92, pp. 7425–7429, August 1995
Neurobiology

Probing the transmembrane topology of cyclic nucleotide-gated ion channels with a gene fusion approach

(channel structure/olfaction/photoreception)

DORIS K. HENN, ARND BAUMANN, AND U. BENJAMIN KAUPP

Institut für Biologische Informationsverarbeitung, Forschungszentrum Jülich, Postfach 1913, 52425 Jülich, Germany

Communicated by Jonathan Beckwith, Harvard Medical School, Boston, MA, April 10, 1995 (received for review February 10, 1995)

ABSTRACT **Cyclic nucleotide-gated (CNG) cation channels contain two short sequence motifs—a residual voltage-sensor (S4) and a pore-forming (P) segment—that are reminiscent of similar segments in voltage-activated Shaker-type K^+ channels. It has been tacitly assumed that CNG channels and this K^+ channel subfamily share a common overall topology, characterized by a hydrophobic domain comprising six membrane-spanning segments. We have systematically investigated the topology of CNG channels from bovine rod photoreceptor and *Drosophila melanogaster* by a gene fusion approach using the bacterial reporter enzymes alkaline phosphatase and β-galactosidase, which are active only in the periplasm and only in the cytoplasm, respectively. Enzymatic activity was determined after expression of fusion constructs in *Escherichia coli*. CNG channels were found to have six membrane-spanning segments, suggesting that CNG and Shaker-type K^+ channels, albeit distant relatives within a gene superfamily of ion channels, share a common topology.**

The topology of a membrane protein is defined by the way it weaves back and forth across the membrane (1). It has been widely accepted that members of the families of ligand-gated and voltage-activated ion channels are characterized by four and six membrane-spanning segments, respectively (2, 3). This simple classification has recently been seriously undermined by cloning of structurally divergent members of these gene families (4, 5) and by functional approaches (6–9). A case in point is the topology of glutamate receptors. At least four different models have been proposed over the past few years, based on epitope mapping, phosphorylation studies, electrophysiological properties, and mapping of agonist binding sites (for review, see ref. 10). By systematically introducing artificial glycosylation sites into a member of the glutamate receptor family, Hollmann *et al.* (10) were able to show that previous models were not correct. These studies emphasize the need to systematically examine the topology by independent and more direct methods.

Cyclic nucleotide-gated (CNG) channels are particularly intriguing because they may combine structural features of both voltage- and ligand-activated channels. Based on partial sequence similarity to K^+ channels (11, 12) and glycosylation sites (13) and on hydrophobicity profiles, a model for the transmembrane topology of CNG channels has been proposed that consists of six membrane-spanning segments (S1–S6) and a pore-forming (P) region between S5 and S6 (13–16). However, the hydrophobicity profiles of CNG channels are much less pronounced than those of K^+ channels and do not allow the unambiguous identification of membrane-spanning segments. With various algorithms only two or three hydrophobic regions are classified as membrane-spanning segments. Moreover, the topology of Shaker-type K^+ channels has not been systematically examined by direct experimental approaches, and the popular model is also largely based on hydropathy analysis.

In their pioneering work, Manoil and Beckwith (17, 18) developed a gene fusion approach to study the topology of proteins in the inner membrane of bacteria. This approach is based on the ability of membrane-spanning segments to serve as signal peptides for the export of bacterial reporter enzymes that are active either only in the periplasm or only in the cytoplasm (for review see ref. 19). While this technique has been successfully applied to study bacterial membrane transporters, it has only recently been adopted to examine the topology of eukaryotic membrane receptors (20).

We chose this approach to determine the topology of CNG channels from bovine rod photoreceptors (brCNGC) and from *Drosophila melanogaster* (DmCNGC). We provide evidence that CNG channels embody six membrane-spanning segments, including the S4 segment. These results demonstrate that the gene fusion approach provides a versatile and powerful tool to study the topology of eukaryotic ion channels.

MATERIALS AND METHODS

Fusion Constructs. brCNGC cDNA was cloned in-frame to the coding sequence for the first 11 aa of the LacZ α peptide of the pUC18 vector (Pharmacia). For DmCNGC constructs the cDNA was cloned in-frame to the coding sequence for the first 20 aa of the LacZ α peptide of the pBluescript vector (Stratagene). For alkaline phosphatase (AP) constructs the *phoA* gene was isolated from the pSWFII vector (21) by *Xba* I digestion. This fragment was ligated to CNG channel cDNA into which *Xba* I recognition sites had been introduced by PCR at the respective fusion sites. For β-galactosidase (βGal) constructs an *Xba* I recognition site was introduced into the 5′ part of the open reading frame of the *lacZ* gene. A fragment encompassing the entire coding region was obtained by cutting at the novel *Xba* I site and a *Hin*dIII site and ligated to the channel genes. brS5 was obtained after transposon mutagenesis with Tn*phoA* (17). Aspartate residues in the S3 segment of brS3, brP, DmS3, and DmS5 were exchanged for valine(s) by PCR (22). AP sandwich constructs (21) were obtained by introducing unique *Xba* I and *Hin*dIII recognition sites into the channel genes; the bacterial *phoA* gene was ligated in-frame to these sites.

Expression of Fusion Constructs. Fusion constructs were expressed in *Escherichia coli* CC118 (17), which lacks endogenous AP and βGal activity. Single colonies harboring AP constructs were grown in Luria–Bertani (LB) medium supplemented with 1% glucose for 6 hr at 37°C before determination of enzymatic activity. For the induction of brCNGC

The publication costs of this article were defrayed in part by page charge payment. This article must therefore be hereby marked "*advertisement*" in accordance with 18 U.S.C. §1734 solely to indicate this fact.

Abbreviations: AP, alkaline phosphatase; βGal, β-galactosidase; CNG, cyclic nucleotide-gated; DmCNGC, CNG channel of *Drosophila melanogaster*; brCNGC, CNG channel of bovine rod photoreceptor; EL*n*, extracellular loop *n*; IL*n*, intracellular loop *n*; P region, pore-forming region; S*n*, membrane-spanning segment *n*; HI, hydrophobicity index.

constructs, glucose was omitted from the medium 4 hr after inoculation and incubation was continued at 37°C for 2 hr. βGal constructs were grown overnight. AP and βGal enzymatic activity was determined essentially as described (23, 24).

Western Blot Analysis. Cytoplasmic, membrane, and periplasmic fractions of bacterial extracts were obtained as described (18). Proteins were separated by SDS/PAGE and AP was detected with the monoclonal antibody V1AP1 (Medac, Hamburg, Germany). Immunoreactivity was visualized with the ECL detection kit (Amersham).

RESULTS

Hydrophobicity Analysis of brCNGC and DmCNGC. Only two of seven hydrophobic regions in brCNGC (Fig. 1 *Upper*, regions 4 and 5) and three of seven hydrophobic regions in DmCNGC (Fig.1 *Lower*, regions 1, 4, and 5) are classified as transmembrane segments according to the Kyte and Doolittle criterion (ref. 25; peak HI ≥ 1.6). Another hydrophobic region in the C-terminal part fulfills this criterion but harbors the cGMP-binding site (26) and therefore does not span the membrane. Most importantly, the hydrophilic S4 segment is not required to traverse the membrane for functional reasons as in voltage-activated K^+ channels, because CNG channels are not activated by voltage. This analysis illustrates that the model shown in Fig. 2 cannot be deduced from hydrophobicity profiles of CNG channels.

Fusion Constructs of brCNGC. We systematically studied the ability of each candidate membrane-spanning segment (see Fig. 2) of CNG channels to export bacterial reporter enzymes (18, 27). Progressively 3′-truncated cDNAs of brCNGC and DmCNGC were fused to one of two bacterial genes—*phoA*, coding for AP, or *lacZ*, coding for βGal—and were expressed in *E. coli*. The C-terminal ends of putative extra- and intracellular loops (EL and IL; see Fig. 2) were chosen as fusion sites, because hydrophilic linkers between membrane-spanning segments codetermine their own localization (19, 28). AP is active only in the periplasm, where intrachain disulfide bonds can form (29). The results obtained with AP fusions were corroborated by fusions containing βGal, which is active only in the cytoplasm. This approach allowed us not only to identify membrane-spanning segments but also to determine their orientation in the membrane. The fusion constructs and values for reporter enzyme activity are summarized in Table 1.

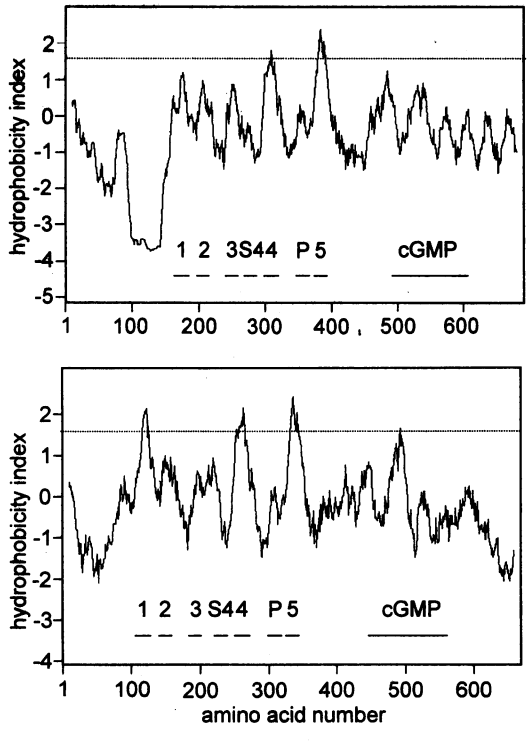

FIG. 1. Hydrophobicity plots of brCNGC (*Upper*) and DmCNGC (*Lower*) polypeptides. The hydrophobicity index (HI) was calculated by the method of Kyte and Doolittle (25) and plotted against the amino acid number, with a window size of 19 aa. The dotted line indicates a HI of 1.6. Hydrophobic regions (numbered 1–5), the residual voltage-sensor (S4) motif, the P region, and the cGMP-binding site are indicated by horizontal bars.

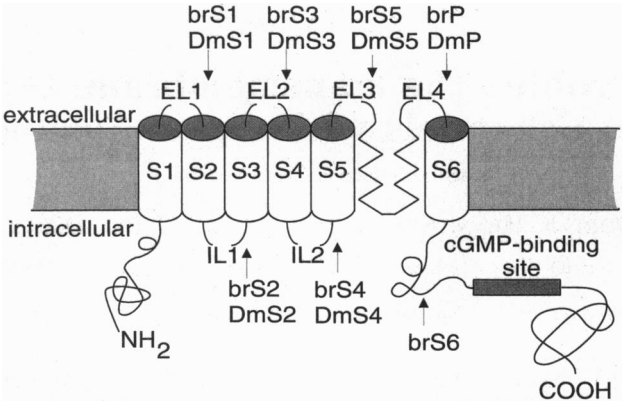

FIG. 2. Proposed model of the two-dimensional architecture of CNG channels. Extracellular (EL) and intracellular (IL) loops of the channel polypeptides are labeled. Positions of fusion junctions to AP or βGal (see Table 1) are indicated by arrows.

AP fusions to EL3 and EL4 of brCNGC (brS5 and brP) were active, whereas the corresponding βGal fusions were inactive. Moreover, AP fusions to IL2 (brS4) and after S6 (brS6) were inactive, whereas the respective βGal fusions were highly active. AP fusions to EL1 (brS1) and EL2 (brS3) were inactive, while the corresponding βGal fusions were active. These results identify only S5 and S6 of the brCNGC as membrane-spanning segments.

Fusion Constructs of DmCNGC. AP fusions to EL1, EL3, and EL4 of DmCNGC (DmS1, DmS5, and DmP) were highly active; the corresponding βGal fusions were inactive. AP fusions to IL1 (DmS2) and IL2 (DmS4) were inactive, whereas βGal fusions to the same sites were highly active. These results identify S1, S2, S5, and S6 of the DmCNGC as membrane-spanning segments. AP fusions to EL2 (DmS3) were inactive, as was observed for brS3.

Fusion Constructs Mutated in S3. There is precedent that charged amino acid residues in signal peptides of prokaryotic secretory proteins severely impair the export efficacy (30, 31). The S3 segments that do not behave as export signals from either channel carry two aspartate residues (D247 and D255 in brCNGC; D191 and D199 in DmCNGC). We suspected that these residues also impair the export efficacy of S3 segments in the fusion constructs. After replacement of either one of these acidic residues with a neutral hydrophobic residue, valine, in DmCNGC (DmS3-D191V; DmS3-D199V), previously inactive AP fusions became highly active (≥100-fold increase in activity; Table 2). When both aspartates were neutralized by replacement with valine (DmS3-D191/199V), the AP activity increased even further. Similarly, neutralization of one aspartate in S3 of brCNGC (brS3-D255V) also yielded active AP fusions.

The activities of the respective mutated βGal fusions (brS3-D255V and DmS3-D199V) were significantly reduced compared with those of the nonmutated constructs. However, the residual βGal activity (Table 2) indicated that the mutated S3 segments were still poor export signals for the large βGal moiety.

Table 1. Enzyme activity of fusions with brCNGC and DmCNGC

Fusion	Fusion site	Reporter enzyme	Enzymatic activity, units
brS1	Y194	AP	8.5 ± 0.8 (7)
		ßGal	3670 ± 103 (6)
brS2	R232	AP	5.9 ± 0.5 (7)
		ßGal	2536 ± 73.0 (6)
brS2sand	R232	AP	6.9 ± 10.0 (5)
brS3	F261	AP	5.0 ± 0.8 (7)
		ßGal	1724 ± 55.3 (6)
brS4	I295	AP	5.7 ± 1.2 (7)
		ßGal	1733 ± 58.6 (6)
brS5	Y352	AP	2461 ± 390 (7)
		ßGal	n.c.
brP	D370	AP	297 ± 19.1 (7)
		ßGal	295 ± 18.5 (6)
brPsand	D370	AP	112 ± 8.0 (7)
brS6	T471	AP	2.3 ± 0.6 (5)
		ßGal	4791 ± 685 (6)
boS1	Y171	AP	44.7 ± 2.5 (8)
		ßGal	203 ± 39.6 (5)
DmS1	A138	AP	2766 ± 290 (6)
		ßGal	31.3 ± 10.4 (6)
DmS2	Y182	AP	4.1 ± 2.5 (4)
		ßGal	6791 ± 657 (5)
DmS3	C217	AP	7.3 ± 2.7 (4)
		ßGal	6966 ± 1101 (6)
DmS4	F249	AP	6.7 ± 2.1 (6)
		ßGal	3863 ± 830 (6)
DmS5	L287	AP	247 ± 129 (2)
		ßGal	18.9 ± 6.7 (6)
DmP	N321	AP	246 ± 76.3 (4)
		βGal	27.7 ± 10.2 (5)

Values of enzymatic activity (mean ± SEM) for different fusion constructs are listed. The number of experiments is given in parentheses. A pictograph of the construct is shown in front of each line; filled circles represent the reporter enzyme moiety. In fusion designations, br refers to bovine rod, and bo to bovine olfactory epithelium, Dm to *D. melanogaster* CNG channel fusions; S1–S6 indicate the transmembrane segment in front of the reporter enzyme AP or βGal; "sand" refers to sandwich fusions (see text); P refers to fusions behind the P region. n.c., Not constructed. The last amino acid residue of the channel polypeptide in front of the reporter enzyme is indicated as fusion site. Fusions with AP activity <10 units and βGal activity <300 units are considered as inactive.

Neutralization of charged residues might artificially create a new transmembrane domain and thereby might reverse the orientation of segments located downstream of the mutation. In fact, deletion of membrane-spanning segments can reverse the orientation of the downstream part of a polypeptide (32).

Table 2. Enzyme activity of fusions mutated in segment S3

Fusion	Fusion site	Reporter enzyme	Enzymatic activity, units
brS3	F261	AP	5.0 ± 0.8 (7)
		ßGal	1724 ± 55.3 (6)
brS3-D255V	F261	AP	173 ± 24.8 (5)
		ßGal	1262 ± 63.0 (6)
brP	D370	AP	297 ± 19.1 (7)
		ßGal	295 ± 18.5 (6)
brP-D255V	D370	AP	264 ± 11.9 (5)
		ßGal	4.2 ± 4.2 (6)
DmS3	C217	AP	7.3 ± 2.7 (4)
		ßGal	6966 ± 1101 (6)
DmS3-D191V	C217	AP	967 ± 196 (5)
		ßGal	n.c.
DmS3-D199V	C217	AP	619 ± 102 (5)
		ßGal	1007 ± 395 (6)
DmS3-D191/199V	C217	AP	1475 ± 451 (6)
		ßGal	n.c.
DmS5	L287	AP	247 ± 129 (2)
		ßGal	18.9 ± 6.7 (6)
DmS5-D199V	L287	AP	214 ± 11.5 (2)
		ßGal	8.9 ± 9.6 (4)
DmS5-D191/199V	L287	AP	181 ± 7.0 (2)
		ßGal	n.c.

Abbreviations are as in Table 1. Filled squares indicate the mutated aspartate residues in S3.

We tested this possibility by probing the orientation of S5 in mutants in which one or both aspartates in S3 were neutralized (DmS5-D199V, DmS5-D191/199V, and brP-D255V). These constructs still yielded AP activities similar to those of the nonmutated fusions. Thus, the mutations specifically enhance the export efficacy of S3 while preserving the orientation of the following membrane segments. Although these results suggest that S3 and thereby also S4 of brCNGC and DmCNGC represent membrane-spanning segments, they do not rigorously exclude two alternative interpretations. Downstream signals, if strong enough, can counteract the effect of upstream topogenic signals (32); creating a new S3 does not necessarily change the orientation of segments S5 and S6. If the mutations make segment S3 a good export signal, this could artificially lead to segment S4 being also pulled into the membrane and acting as a stop–transfer sequence. We therefore constructed "sandwich" fusions, brS3sand and DmS3sand, in which AP was inserted between S3 and S4. Unfortunately, these constructs were inactive (see *Discussion*).

Export Efficacy of S1 Correlates with Hydrophobicity. The previous results tentatively identify six membrane-spanning segments in DmCNGC but only four in brCNGC. S1 of brCNGC, which fails to export AP, is not very hydrophobic (HI ≈ 1.4), in contrast to S1 of DmCNGC (HI ≈ 2.3), which efficiently exports AP. To test the hypothesis that hydrophobicity is a critical determinant of export efficacy, we constructed AP- and βGal fusions to S1 of the CNG channel from bovine olfactory epithelium (boCNGC; ref. 33). The HI of boS1 (≈1.9) is intermediate between that of brCNGC and

DmCNGC. The activity of the AP fusion of boS1 was 5-fold higher and the activity of the respective βGal fusion was almost 20-fold lower than the corresponding fusion constructs from brS1 (Table 1). This result suggests that the ability of segment S1 to serve as a signal peptide depends critically on its hydrophobicity and supports the idea that S1 in fact is a membrane-spanning segment in CNG channels.

Western Blot of Fusion Proteins. Expression of AP fusion constructs was examined by Western blot analysis with an AP antibody to exclude the possibility that lack of enzymatic activity resulted from insufficient synthesis of fusion proteins. All active AP fusions (Fig. 3*A*, lanes 2–7) yielded a single band with an apparent M_r of 48,000–50,000, slightly larger than that of native AP (Fig. 3*A*, lanes 1 and 10). This result demonstrates that AP is exported to the periplasm and that active AP fusions are cleaved by proteases. In contrast, inactive AP fusions yielded progressively larger products, with size depending on the site of fusion of AP to the channel polypeptide (Fig. 3*A*, lanes 11–17). Inactive AP fusions also gave rise to additional bands of smaller sizes, indicating that the fusion proteins had been partially degraded by proteolysis either because of incomplete insertion into the membrane or because of incorrect folding of the expressed polypeptide.

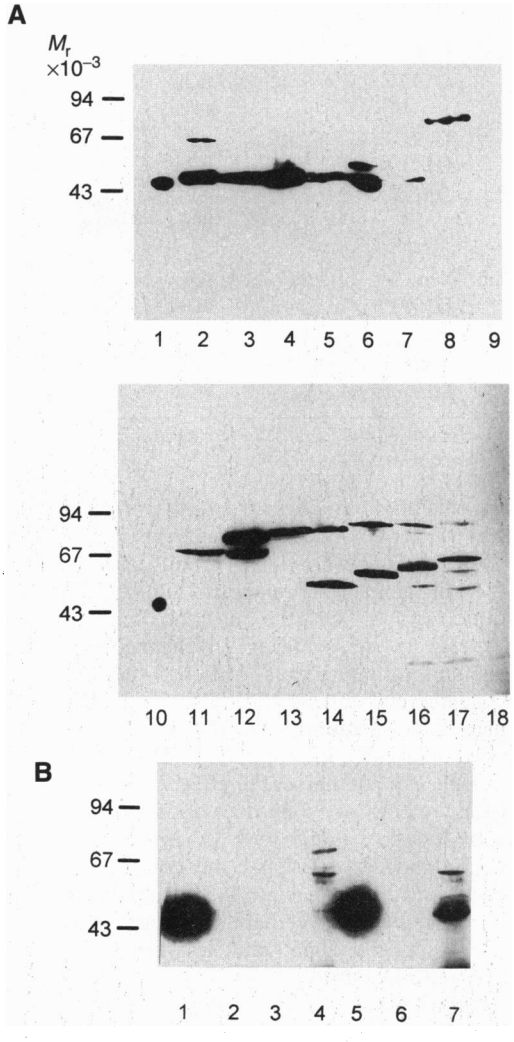

FIG. 3. Western blot analysis of the expression of AP fusions. (*A*) Lanes 1 and 10, native AP; lanes 2–8 and 11–17, whole-cell extracts of CC118 cells harboring various AP fusion constructs (lane 2, DmS1; lane 3, DmS3-D191/199V; lane 4, DmS3-D191V; lane 5, DmS5; lane 6, brS5; lane 7, brP; lane 8, brPsand; lane 11, DmS2; lane 12, DmS3; lane 13, DmS4; lane 14, brS1; lane 15, brS2; lane 16, brS3; lane 17, brS4); lanes 9 and 18, extracts of nontransformed CC118 cells. (*B*) Lane 1, native AP; lanes 2–4, DmS3; lanes 5–7, DmS3-D191/199V. Lanes 2 and 5, periplasmic fractions; lanes 3 and 6, cytoplasmic fractions; lanes 4 and 7, membrane fractions.

We analyzed the distribution of AP in cytoplasmic, periplasmic, and membrane fractions of bacteria expressing DmS3 and the mutated DmS3-D191/199V construct. As expected, only the active fusion (DmS3-D191/199V) yielded AP in the periplasmic fraction (Fig. 3*B*, lane 5). AP immunoreactivity in membrane fractions was detected from both active and inactive constructs (Fig. 3*B*, lanes 4 and 7). Cytosolic fractions did not contain AP immunoreactivity (Fig. 3*B*, lanes 3 and 6).

DISCUSSION

The validity of the gene fusion approach for the study of eukaryotic membrane proteins rests on three assumptions. The first is that polypeptides in the bacterial host adopt the same topology as in the native membrane. This assumption seems plausible, because secretion of proteins from cells is a ubiquitous process: components of the translocation apparatus are conserved in evolution, and hydrophobic signal sequences that initiate the translocation across membranes are interchangeable between pro- and eukaryotes (34). Moreover, the previous assignment of the N and C termini of brCNGC to the cytoplasmic face (35) and N-glycosylation of asparagine-327 in EL3 of brCNGC (13) are in agreement with the topology determined in this study. Thus, with respect to the S5 and S6 segments and the location of the N and C termini, the topology of the rod CNG channel expressed in bacteria and in the native membrane is the same. The topology of the β-adrenergic receptor was recently probed with the gene fusion approach (20). It was concluded that the polypeptide expressed in bacteria adopted the same topology as in the native membrane.

The second assumption is that topogenic cues are not disrupted in the truncated fusion constructs. Since sandwich fusions (21) between the entire channel polypeptide and AP (brS2sand and brPsand; Table 1) gave results similar to those of the truncated fusion constructs, this assumption is also plausible.

The third assumption is that each membrane-spanning segment behaves as an efficient export signal. This assumption is not generally valid, because S1 of brCNGC and unmutated S3 of both CNG channels failed to export AP. The sequences of brCNGC and DmCNGC are strikingly similar (≈80% sequence similarity; ref. 36), and therefore it is not very likely that the two CNG channel species adopt distinct transmembrane topologies; instead, we assume that S1 of brCNGC is not sufficiently hydrophobic to serve as a signal peptide for the export of a reporter enzyme. This interpretation seems likely in view of the enhanced export efficacy of S1 segments from DmCNGC and boCNGC that are significantly more hydrophobic.

S3, apart from S4, is the least hydrophobic segment (HI ≈ 0.65) and fails to function as export signal unless either one of two negatively charged aspartate residues is neutralized. We suspect that in the native channel these negative charges are compensated by positively charged residues in adjacent segments, perhaps S4, and that both segments are simultaneously inserted into the membrane. In AP fusions the charges would be uncompensated and might inhibit insertion of S3. Because the orientation of downstream segments is not reversed in S3 mutants, we conclude that the mutations did not create a novel transmembrane segment.

However, the orientation of downstream segments would also be preserved if S4 were pulled into the membrane along with S3. This alternative interpretation seems to be much less plausible, because such a mechanism would require that neutralization of a single charge can promote the "unspecific" transfer into the membrane of two segments that normally would be part of a cytoplasmic loop. The increase in hydro-

phobicity of S3 due to a single substitution is rather moderate (DmS3-D191V, HI ≈ 1.0) and even the double mutant of S3 (DmS3-D191/199V; HI ≈ 1.4) is not more hydrophobic than S1 from brCNGC, which in contrast to mutated S3 fails to export AP. Therefore, mutant S3 cannot be considered a strong export signal that would be prone to dragging another segment, and the large increase in AP activity may be only in part caused by the hydrophobic effect. Further, the S4 segment carries six charges and the "pull-along" mechanism would require the net transfer of five additional charges into the membrane, a process that is energetically highly unfavorable.

The loop between S3 and S4 is extremely short, and the steric constraints may not permit AP to form functional dimers in sandwich constructs. This conclusion is supported by the observation that AP activity of sandwich constructs of bacterial transporters (21) and also CNG channels is notoriously lower than in simple AP fusions. Moreover, we do not know of any example where an inactive AP fusion became active in the corresponding sandwich construct. In conclusion, the failure of brS3sand and DmS3sand to express AP activity cannot be taken as evidence that S3 and S4 are located in the cytoplasm. Nevertheless, the experimental support for S3 being a transmembrane segment is not as strong as for the other segments.

The topology model is also consistent with the "positive-inside" rule (1, 30, 37). The cytoplasmic linker IL1 of brCNGC (DmCNGC) carries seven (four) arginine or lysine residues, whereas EL1 and EL2 carry only one (one) and one (zero) positively charged residues, respectively. Finally, all fusions of brCNGC and DmCNGC, except brS1, gave identical results and thus allowed the unambiguous assignment of membrane-spanning segments.

The sequence similarity of the S4 and P segments (11–14) and mutagenesis studies of the P region (38–40) reveal a possible evolutionary connection between ion channels that are as functionally diverse as K^+, Ca^{2+}, and CNG channels. Here we provide evidence that the evolutionary kinship between voltage- and second messenger-gated channels is also reflected in a similar topological architecture characterized by six membrane-spanning segments.

We thank Drs. W. Altenhofen, E. Eismann, M. Klose, and I. Weyand for helpful suggestions on the manuscript and Drs. R. Freudl (Forschungszentrum Jülich) and M. Ehrmann (Universität Konstanz) for initial help with the gene fusion technique and stimulating discussions. This work was supported by the Deutsche Forschungsgemeinschaft.

1. von Heijne, G. (1994) *Annu. Rev. Biophys. Biomol. Struct.* **23,** 167–173.
2. Jan, L. Y. & Jan, Y. N. (1992) *Cell* **69,** 715–718.
3. Jessell, T. M. & Kandel, E. R. (1993) *Cell/Neuron* **72/10** (Suppl.), 1–30.
4. Kubo, Y., Baldwin, T. J., Jan, Y. N. & Jan, L. Y. (1993) *Nature (London)* **362,** 127–133.
5. Ho, K., Nichols, C. G., Lederer, W. J., Lytton, J., Vassilev, P. M., Kanazirska, M. V. & Hebert, S. C. (1993) *Nature (London)* **362,** 31–38.
6. Tingley, W. G., Roche, K. W., Thompson, A. K. & Huganir, R. L. (1993) *Nature (London)* **364,** 70–73.
7. Kuryatov, A., Laube, B., Betz, H. & Kuhse, J. (1994) *Neuron* **12,** 1291–1300.
8. Wo, Z. G. & Oswald, R. E. (1994) *Proc. Natl. Acad. Sci. USA* **91,** 7154–7160.
9. Taglialatela, M., Wible, B. A., Caporaso, R. & Brown, A. M. (1994) *Science* **264,** 844–847.
10. Hollmann, M., Maron, C. & Heinemann, S. (1994) *Neuron* **13,** 1331–1343.
11. Jan, L. Y. & Jan, Y. N. (1990) *Nature (London)* **345,** 672.
12. Heginbotham, L., Abramson, T. & MacKinnon, R. (1992) *Science* **258,** 1152–1155.
13. Wohlfart, P., Haase, W., Molday, R. S. & Cook, N. J. (1992) *J. Biol. Chem.* **267,** 644–648.
14. Goulding, E. H., Ngai, J., Kramer, R. H., Colicos, S., Axel, R., Siegelbaum, S. A. & Chess, A. (1992) *Neuron* **8,** 45–58.
15. Bönigk, W., Altenhofen, W., Müller, F., Dose, A., Illing, M., Molday, R. S. & Kaupp, U. B. (1993) *Neuron* **10,** 865–877.
16. Eismann, E., Bönigk, W. & Kaupp, U. B. (1993) *Cell. Physiol. Biochem.* **3,** 332–351.
17. Manoil, C. & Beckwith, J. (1985) *Proc. Natl. Acad. Sci. USA* **82,** 8129–8133.
18. Manoil, C. & Beckwith, J. (1986) *Science* **233,** 1403–1408.
19. Boyd, D. (1994) in *Membrane Protein Structure: Experimental Approaches*, ed. White, S. (Oxford Univ. Press, New York), pp. 144–163.
20. Lacatena, R. M., Cellini, A., Scavizzi, F. & Tocchini-Valentini, G. P. (1994) *Proc. Natl. Acad. Sci. USA* **91,** 10521–10525.
21. Ehrmann, M., Boyd, D. & Beckwith, J. (1990) *Proc. Natl. Acad. Sci. USA* **87,** 7574–7578.
22. Herlitze, S. & Koenen, M. (1990) *Gene* **91,** 143–147.
23. Brickman, E. & Beckwith, J. (1975) *J. Mol. Biol.* **96,** 307–316.
24. Miller, J. H. (1972) *Experiments in Molecular Genetics* (Cold Spring Harbor Lab. Press, Plainview, NY).
25. Kyte, J. & Doolittle, R. F. (1983) *J. Mol. Biol.* **157,** 105–132.
26. Kaupp, U. B., Niidome, T., Tanabe, T., Terada, S., Bönigk, W., Stühmer, W., Cook, N. J., Kangawa, K., Matsuo, H., Hirose, T., Miyata, T. & Numa, S. (1989) *Nature (London)* **342,** 762–766.
27. Manoil, C., Mekalanos, J. J. & Beckwith, J. (1990) *J. Bacteriol.* **172,** 515–518.
28. von Heijne, G. (1986) *EMBO J.* **5,** 3021–3027.
29. Derman, A. I. & Beckwith, J. (1991) *J. Bacteriol.* **173,** 7719–7722.
30. Allard, J. D. & Bertrand, K. P. (1992) *J. Biol. Chem.* **267,** 17809–17819.
31. Michaelis, S., Inouye, H., Oliver, D. & Beckwith, J. (1983) *J. Bacteriol.* **154,** 366–374.
32. McGovern, K., Ehrmann, M. & Beckwith, J. (1991) *EMBO J.* **10,** 2773–2782.
33. Ludwig, J., Margalit, T., Eismann, E., Lancet, D. & Kaupp, U. B. (1990) *FEBS Lett.* **270,** 24–29.
34. Jungnickel, B., Rapoport, T. A. & Hartmann, E. (1994) *FEBS Lett.* **346,** 73–77.
35. Molday, R. S., Molday, L. L., Dose, A., Clark-Lewis, I., Illing, M., Cook, N. J., Eismann, E. & Kaupp, U. B. (1991) *J. Biol. Chem.* **266,** 21917–21922.
36. Baumann, A., Frings, S., Godde, M., Seifert, R. & Kaupp, U. B. (1994) *EMBO J.* **13,** 5040–5050.
37. von Heijne, G. (1989) *Nature (London)* **341,** 456–458.
38. Root, M. J. & MacKinnon, R. (1993) *Neuron* **11,** 459–466.
39. Eismann, E., Müller, F., Heinemann, S. H. & Kaupp, U. B. (1994) *Proc. Natl. Acad. Sci. USA* **91,** 1109–1113.
40. Yang, J., Ellinor, P. T., Sather, W. A., Zhang, J.-F. & Tsien, R. W. (1993) *Nature (London)* **366,** 158–161.